Informes Técnicos Ciemat

1208
Junio, 2010

Liquid Scintillation High Resolution Spectral Analysis

A. Grau Carles
A. Grau Malonda

Subdirección General de Relaciones Institucionales y Transferencia del Conocimiento

Toda correspondencia en relación con este trabajo debe dirigirse al Servicio de Información y Documentación, Centro de Investigaciones Energéticas, Medioambientales y Tecnológicas, Ciudad Universitaria, 28040-MADRID, ESPAÑA.

Las solicitudes de ejemplares deben dirigirse a este mismo Servicio.

Los descriptores se han seleccionado del Thesauro del DOE para describir las materias que contiene este informe con vistas a su recuperación. La catalogación se ha hecho utilizando el documento DOE/TIC-4602 (Rev. 1) Descriptive Cataloguing On-Line, y la clasificación de acuerdo con el documento DOE/TIC.4584-R7 Subject Categories and Scope publicados por el Office of Scientific and Technical Information del Departamento de Energía de los Estados Unidos.

Catálogo general de publicaciones oficiales
http://www.060.es

Depósito Legal: M -14226-1995
ISSN: 1135 - 9420
NIPO: 471-10-026-0

Editorial CIEMAT

CLASIFICACIÓN DOE Y DESCRIPTORES

S46
SCINTALLATION COUNTING; LIQUID SCINTILLATORS; EFFICIENCY; PHOTOMULTIPLIERS; SCINTILLATION COUNTERS; MATHEMATICAL MODELS; DISTRIBUTION FUNCTIONS.

Liquid Scintillation High Resolution Spectral Analysis

Grau Cales, A.; Grau Malonda, A.
28 pp. 20 fig. 107 refs.

Abstract:
The CIEMAT/NIST and the TDCR methods in liquid scintillation counting are based on the determination of the efficiency for total counting. This paper tries to expand these methods analysing the pulse-height spectrum of radionuclides. To reach this objective we have to generalize the equations used in the model and to analyse the influence of ionization and chemical quench in both spectra and counting efficiency. We present equations to study the influence of different photomultipliers response in systems with one, two or three photomultipliers. We study the effect of the electronic noise discriminator level in both spectra and counting efficiency. The described method permits one to study problems that up to now was not possible to approach, such as the high uncertainty in the standardization of pure beta-ray emitter with low energy when we apply the TDCR method, or the discrepancies in the standardization of some electron capture radionuclides, when the CIEMAT/NIST method is applied

Análisis de Espectros de Alta Resolución en Centelleo Líquido

Grau Cales, A.; Grau Malonda, A.
28 pp. 20 fig. 107 refs.

Resumen:
Los métodos CIEMAT/NIST y TDCR en centelleo líquido se basan en la determinación de las eficiencias totales de recuento. En el presente trabajo se trata de ampliar estos métodos analizando los espectros de amplitud de los impulsos. Ello requiere la generalización de las expresiones de cálculo y permite analizar la influencia de las extinciones por ionización y química tanto en el espectro como en la eficiencia de recuento. Se desarrollan expresiones para el estudio de la influencia de la diferente respuesta de los fotomultiplicadores en sistemas con 1, 2 ó 3 fotomultiplicadores Se analiza la influencia del nivel del discriminador del ruido electrónico en el espectro y en la eficiencia de recuento. El método descrito permite estudiar problemas que hasta ahora no era posible abordar, tales como la elevada incertidumbre en la calibración de emisores beta de baja energía con el método TDCR, o las discrepancias en la calibración de algunos nucleidos que se desintegran por captura electrónica pura cuando se aplica el método CIEMAT/NIST.

Contents

1. Introduction

Liquid scintillation counting has become a universal method for radionuclide standardization. Due to the great advantage that represents the absence of self absorption and the possibility of correcting by well established procedures both ionization and chemical or colour quenching it has been possible to develop accurate computation models.

Two methods compete in the activity determination of radioactive samples: CIEMAT/NIST and TDCR (Triple Double Counting Rate). The first one requires to obtain the counting efficiency of a tracer, usually tritium, and to calculate, by means of a model, the counting efficiency vs. the free parameter for tritium and the radionuclide to be standardized [1-5]. The TDCR requires to measure the radionuclide both in three and two coincidence photomultipliers and to calculate the ratio between the counting rates. A computation model allows one to calculate the counting efficiency vs. the triple and double counting rate and consequently to standardize directly the radionuclide [6-10].

A great volume of work has been carried out in radionuclide standardization [11, 48]. The most complete revision on measurement procedures, with abundant references, is given in [47]. Other works in the same line are given in [48, 49].

Many programs to compute the counting efficiency based in different models have been published [50-64], but no one of them allows us to calculate the radionuclides spectra.

The analysis of experimental liquid scintillation spectra, obtained with two coincident photomultipliers, has been applied very little, in spite of the demonstrated capacity for radioactivity determination in radionuclide mixtures. The most tested and satisfactory method is the Grau Carles method [65-76] based on the deconvolution of spectra. It has been applied to the decomposition of mixtures up to 10 radionuclides. Some of these mixtures like that of ^{14}C and ^{35}S with very close maximum beta energy [66] were considered impossible to obtain the activity of each radionuclide.

Liquid scintillation counting systems permits to develop applications that present advantages with regards to other standardization methods: long half lives with uncertainties lower than other methods [77, 78]; beta spectra shape factor [79-82]; analysis of basic aspects of scintillation process and electron interaction with the scintillator [87-89]; analysis of problems related with the TDCR method [90-93] or with branching ratio determination [93].

In this paper we develop a procedure to calculate the spectra obtained with high resolution spectrometers. We compare the computed and the experimental spectrum for ^{55}Fe obtained with two photomultipliers working in coincidence. We analyse the spectrum of ^{55}Fe when this radionuclide is measured with 1, or 2 or 3 photomultipliers working in coincidence. The procedure is general and can be applied to any radionuclide decaying by beta-ray emission or by electron capture.

Different problems without solution in the standardization of radionuclides by liquid scintillation counting can be approached applying the technique here described.

2. Spectrometers with a single photomultiplier

2.1 Single electron ("mono") pulse-height spectrum

In order to investigate the pulse-height distributions, the spectrum of minimum reaction of a photomultiplier, i.e. of the single photoelectrons ("monos"), must be considered. It is generated by irradiating the photocathode directly by some weak source of incandescent light. The energy of one photon is not enough to produce more than one photoelectron. Fig. 1 shows a typical "mono" spectrum obtained by a RCA 8850 [94]. This photomultiplier has a first dynode made of GaP(Cs) with a high quantum yield which increases the amplification of the first stage.

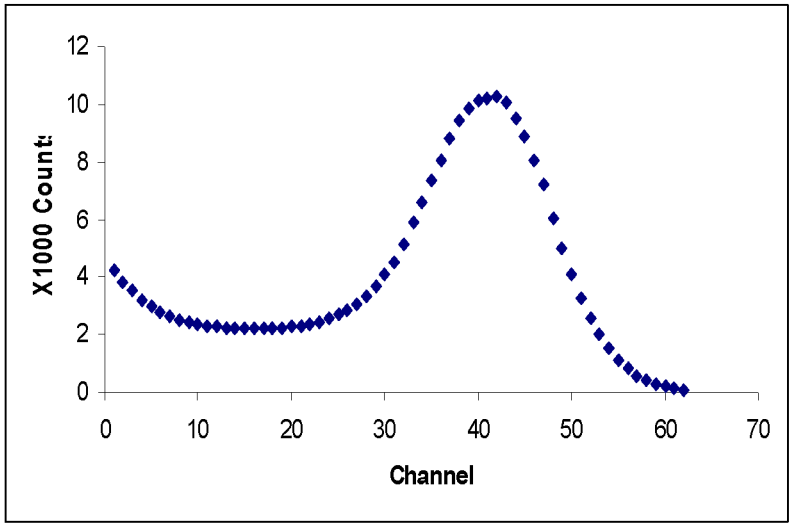

Fig 1.- Spectrum of monos of a RCA 8850 photomultiplier specially selected by its spectral response.

The typical "mono" spectrum can be split up into two parts: a nearly Gaussian peak and a remainder, the origin of which, according to Coates [95], is due to "edge effects". The noise of the photomultiplier and the Gaussian peaks are clearly separated by a valley. This is not the case for some high resolution photomultipliers in which the noise and Gaussian peaks are very close as it is shown in [96]. In this situation we can have a valley below the noise or perhaps only the noise and a Gaussian peak. As we will mention later either of this situations must be clarified to obtain accurate radionuclide standardization. Other photomultipliers, with low resolution, show a half Gaussian pulse distribution and noise. This situation will be not considered in this paper.

2.2 Pulse-height distribution

The pulse-height spectrum from a simple photomultiplier can be considered as a weighted sum over n distributions which correspond to the simultaneous arrival of n monos. When $y_i^{(1)}$ is the monos distribution and $y_i^{(2)}$ the distribution due to two electrons emitted by the photocathode we have:

$$y_i^{(2)} = \sum_{k=1}^{n} y_k^{(1)} y_{i-k}^{(1)} \tag{1}$$

with the condition $i-k \geq 1$. When the number of channels of $y_i^{(1)}$ is N, the number for $y_i^{(2)}$ will be $2N$. When $y_i^{(1)}$ is normalized to 1, we have

$$\sum_{i=1}^{\infty} y_i^{(1)} = 1 \tag{2}$$

then $y_i^{(2)}$ is also normalized to 1. When the number of photoelectrons emitted by the photocathode is 3, the pulse-height distribution is

$$y_i^{(3)} = \sum_{k=1}^{n} y_k^{(1)} y_{i-k}^{(2)} \tag{3}$$

also normalized to 1. The emission of n photoelectrons by the photocathode is given by the distribution

$$y_i^{(n)} = \sum_{k=1}^{n} y_k^{(1)} y_{i-k}^{(k-1)} \tag{4}$$

This equation permits to obtain the electron distribution for $n = 2, 3, \ldots$ due to uniform energy emissions. Fig. 4 shows these distributions for $n = 1, 2, \ldots, 7$, obtained from the monos distribution presented in Fig.1. The curious shape of $y_i^{(2)}$ and $y_i^{(3)}$ is due to the asymmetry of $y_i^{(1)}$. When n increases, spectra become symmetric and the centre of the peak is placed at n times the mean height of the $y_i^{(1)}$ spectrum.

In the case of a single photomultiplier and a source emitting electrons with uniform energy, the pulse-height distributions is given by the equation

$$S_i(m) = \sum_{n=1}^{\infty} \frac{m^n e^{-m}}{n!} y_i^{(n)} \tag{5}$$

where n is the number of electrons emitted by the photocathode following a Poisson statistical distribution with mean m. When E is the interacting electron energy, $Q(E)$ is the ionization quench factor and λ is the free parameter [100], the mean number of electrons at the photocathode is given by:

$$m = \frac{E \times Q(E)}{\lambda} \tag{6}$$

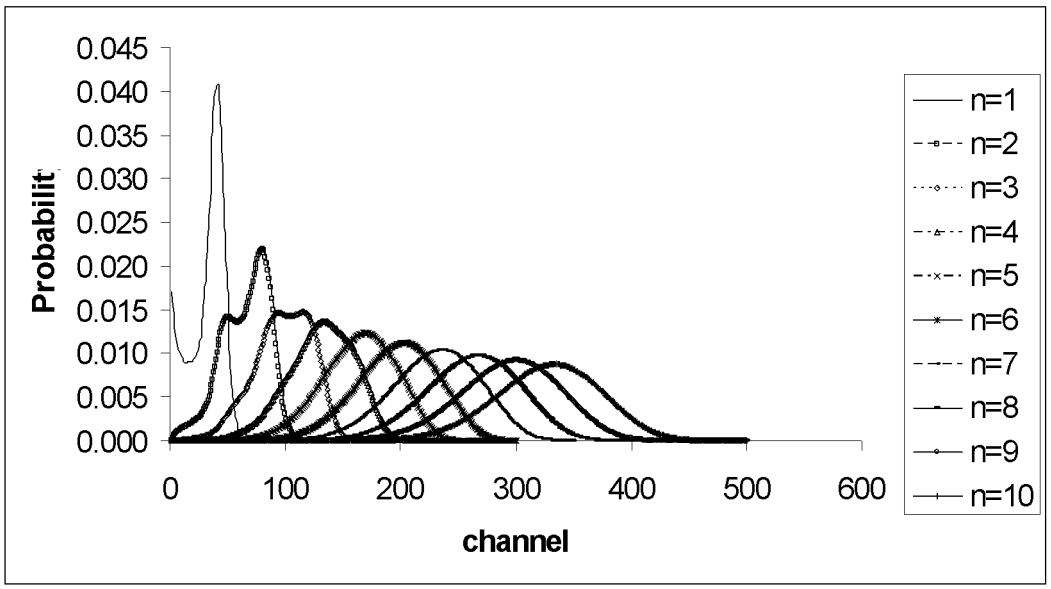

Fig 2.- Spectral photomultiplier response for $n = 1, 2, ...,10$ electrons. For $n > 1$ the response has been computed by the deconvolution of the spectrum of monos given in Fig. 1. We must emphasise the presence of two clear peaks.

where $E \times Q(E)$ is the particle effective energy. Fig. 3 shows spectra for seven monoenergetic emissions with electron means $m = 1, 2, 3, 4, 5, 7$ and 10. For $m = 1$ and 2 the monos is the predominant peak. For $m = 4$, predominant peaks are for 2 and 3 electrons. For $m = 10$ we have only a broad peak. It is important to point up that for low energy electrons, the position of the peaks in the pulse-height spectra are not related with the energy of the interacting electrons. Here the electron energy modulates or acts statistically as a weight for the different peaks.

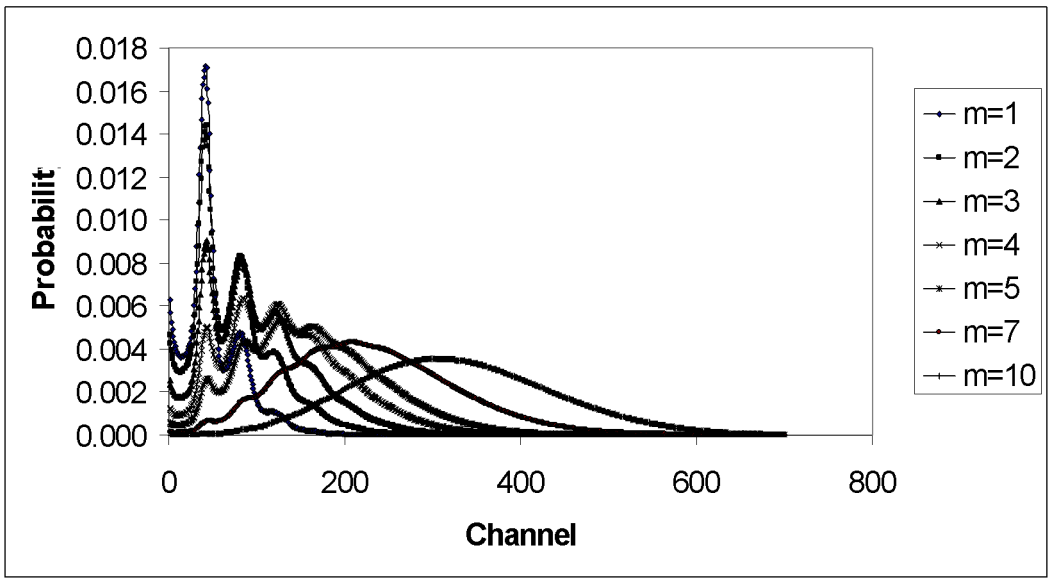

Fig 3.- Emission spectra due to a monoenergetic radiation. The mean number of the electrons at the output of the photocathode is $m = 1, 2, 3, 4, 5, 7, 10$.

The pulse-height spectrum is defined by a series given by:

$$S_i = \sum_{n=1}^{\infty} a_n y_i^{(n)} \qquad (7)$$

where i the channel number in the spectrum. This infinite summation must be truncated and the maximum value of n will depends on the problem. As a general rule, the number of spectral components will be the necessary to obtain the experimental counting efficiency of the problem. In other words, the accuracy of the counting efficiency fixes the number of spectral components.

2.3 Spectrum of ^{55}Fe

^{55}Fe is a radionuclide decaying by pure electron capture with emission of X-rays and Auger electrons of low energy. Fig. 4 shows the computed and experimental spectrum of ^{55}Fe obtained for a RCA 8850 selected by its high resolution [94]. The main discrepancies between experimental and computed spectrum are the following: difference between the heights of the first peak due to one electron emission and different response en the valley. The difference between peaks is due to the after-pulses [98]. To quantify the number of after-pulses in a spectrum is a difficult matter, however in this case the number of after-pulses is 12%. As the after-pulses are accumulated at low energies, the resolution has been modified and the peak is shifted to low energies.

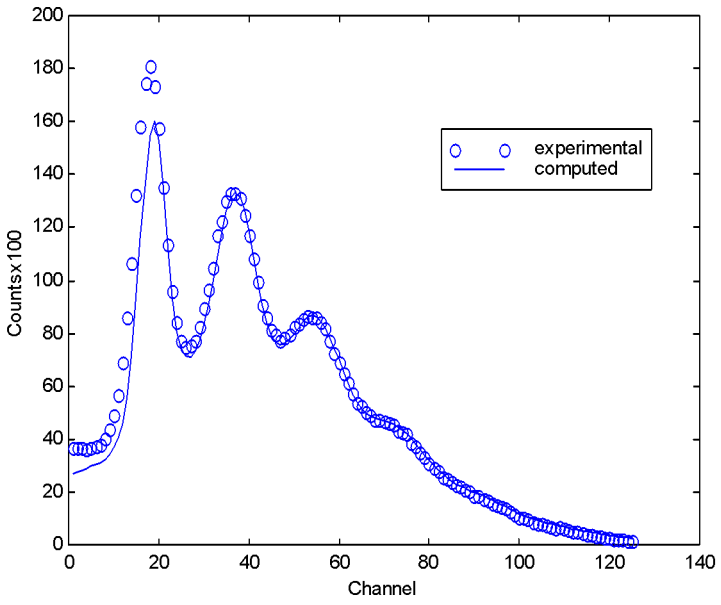

Fig 4.- Experimental and computed spectra of ^{55}Fe for the photomultiplier RCA 8850. The spectrum of monos is given in Fig. 1.

It is interesting to analyse the differences between the region of the spectrum previous to the first peak. The experimental spectrum shows an almost flat component whereas in the calculated one a minimum is observed with an increase of counts in the first channel. This difference is due to the discriminator that eliminates the noise of the

photomultiplier and distorts the spectrum. In this case the problem is not important, but for systems with two or three photomultipliers in coincidence it must be taken into account to obtain the counting efficiency. This effect will be analysed with more detail in other paragraph.

It is observed that both the second peak and the following ones fit perfectly in both spectra.

2.4 Free parameter and kB

We have applied a value of 1.32 keV/electron for the free parameter in the calculation of ^{55}Fe spectrum. The free parameter is directly related with the chemical quenching level in the sample as well as the light looses from the emission of the photocathode. Fig. 5 shows the spectra calculated for λ=1.32, 2.32, 3.32, 5.32, and 10.32 keV/electron, which correspond to increasing chemical quench. For $\lambda = 1.32$ keV/electron we distinguish up to five peaks. The first and the second peaks are the most intense. When chemical quench increases (λ increases) the spectrum is loosing counts in the superior part while the first and the second peaks increases. Chemical quench reduces the pulse-height distribution and consequently the spectrum seems to shrink. However, the peaks don't move, what diminish or increase is the height of them.

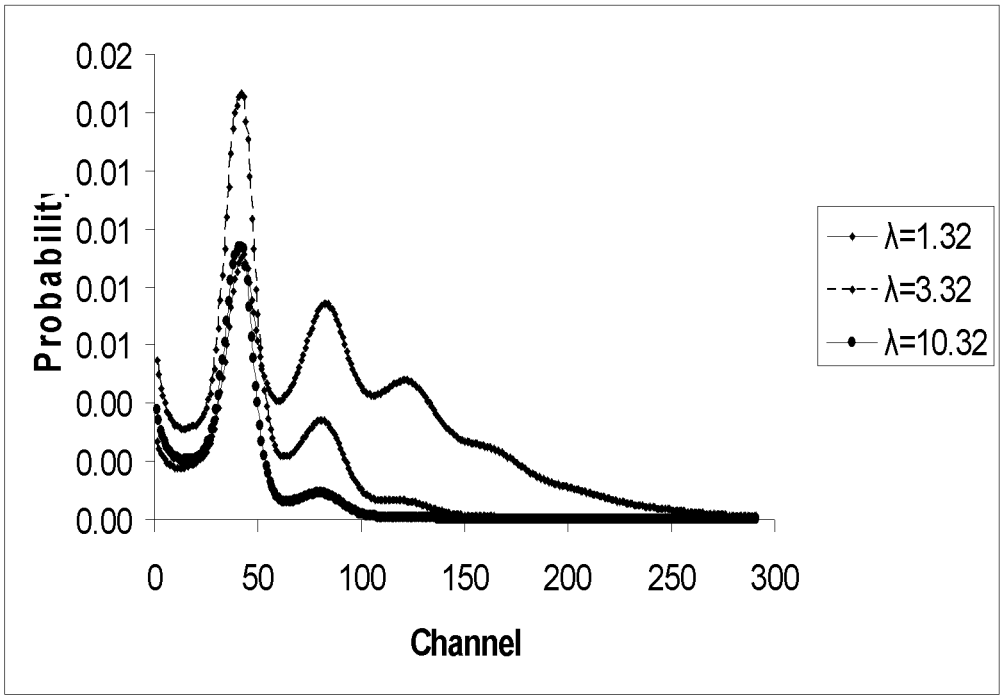

Fig. 5.- ^{55}Fe spectrum for increasing values of the free parameter λ

The kB value introduced to correct for ionization quench has been analyzed in several papers [99-105]. Fig. 6 shows the spectra for three values of the kB, 0.0075, 0.009 and 0.012 cm/MeV. The free parameter value has been fixed in $\lambda = 1.32$ keV/electron in all our computations. The second peak (emission of two photoelectrons)

is practically the same for the three kB values. However, the first peak increases in intensity when the kB increases while the 3 and 4 peaks diminish as kB increases.

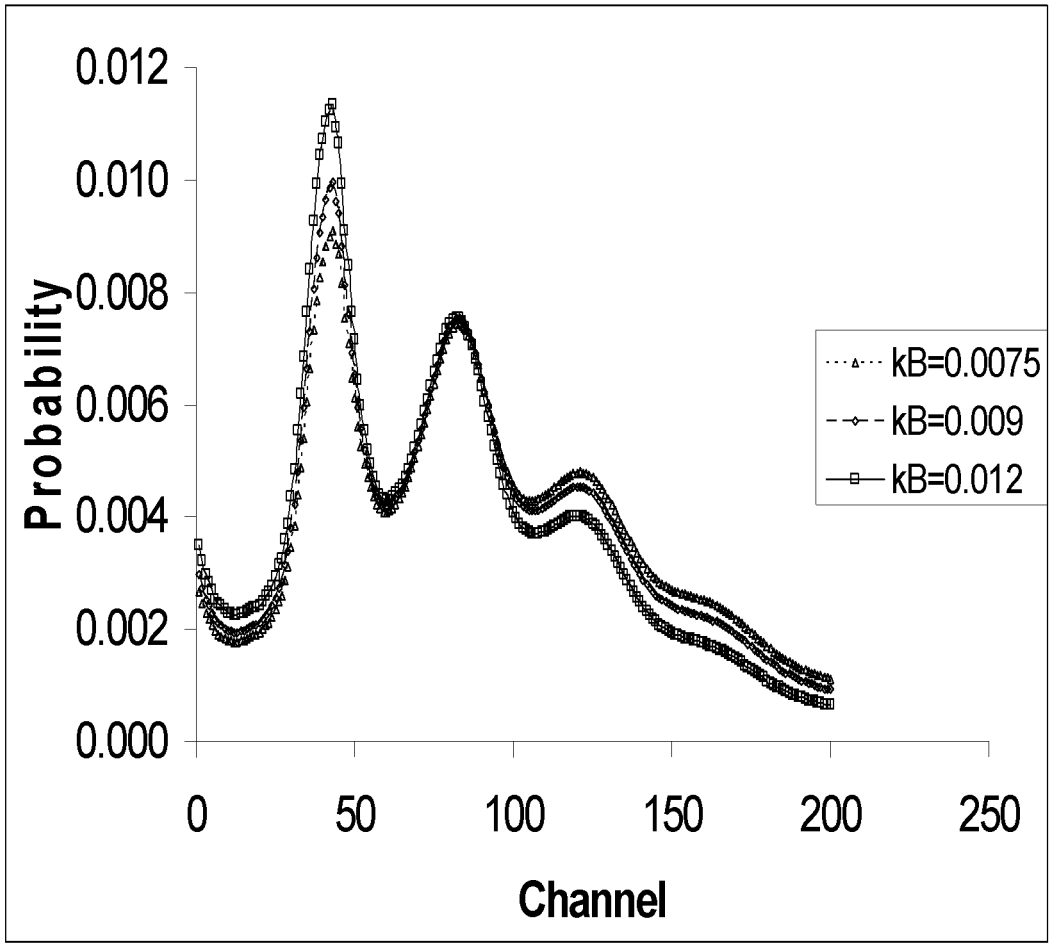

Fig. 6.- ^{55}Fe spectra for three different values of kB

The question arising is the following: is it possible to obtain the same spectrum combining values of kB and values for the free parameter? The answer is positive. Fig. 7 shows two spectra (indistinguishables) obtained with the following values: kB=0.0075 cm/MeV and $\lambda = 1.5$ keV/electron and kB=0.014 cm/MeV and $\lambda = 1.4$ keV/electron, respectively. The counting efficiency is the same in both cases (0.807).

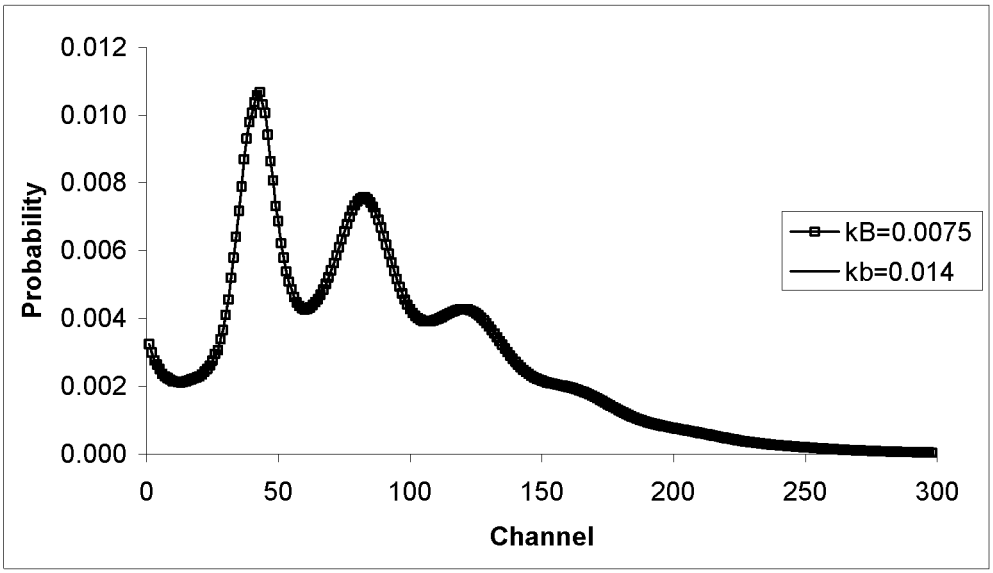

Fig. 7.- ^{55}Fe spectra for two different values of kB and the free parameter: $kB = 0.0075$ cm/MeV and $\lambda = 1.50$ keV/electron and $kB = 0.014$ cm/MeV and $\lambda = 1.40$ keV/electron.

2.6 Spectra of ^{3}H and ^{55}Fe

Fig. 8 shows the computed spectra of ^{3}H and ^{55}Fe for a single photomultiplier. It is observed that although particle emission spectrum of both radionuclides is different: ^{3}H has a continuous spectrum and ^{55}Fe has a discrete one, the output of the photomultiplier is similar in form as was mentioned before.

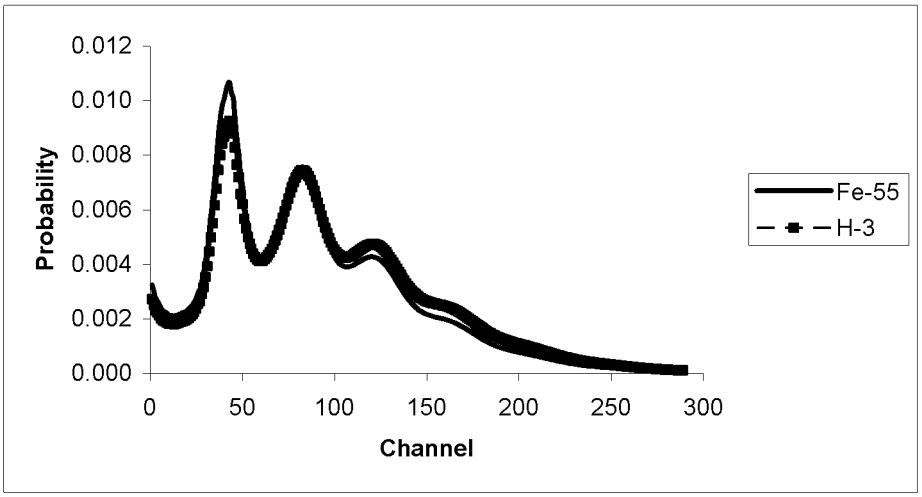

Fig. 8.- Spectra of ^{3}H and ^{55}Fe. The position of the peaks is the same and the heights ones different.

A controversy exists in relation with the optimal tracer in the CIEMAT/NIST method. Some authors use ^{3}H [1, 2] and others ^{55}Fe [106]. It is thought that tritium is a better tracer for beta emitters and ^{55}Fe for electron capture decaying nuclides. This is a logical conclusion when spectra with poor resolution are analyzed and we take into account the disintegration way. However, the question is: Why both radionuclides are good tracers for both forms of disintegration? The spectra in Fig. 8 explain clearly this last fact. The spectral forms produced by the photomultiplier for both disintegration ways are structurally similar.

On the other hand, these spectra explain another important question: Why these tracers allow to calculate the counting efficiency of radionuclides with higher energies? The application of the tracer method in others detectors, e.g. proportional counters, imposes the condition of similar energy particles in both radionuclides. The problem for the standardization of radionuclides by liquid scintillation resides in the non linear response to low energy (below 10 keV) due to ionization quench [99]. The photomultiplier response in low energy is similar for all the radionuclides emitting electrons. The energy of the electrons emitted by the radionuclide only modulates the intensity of the spectral peaks but don't have any influence on the position of the peaks. Fig. 9 shows the spectrum of ^{125}I. We observe that for low energies the spectrum is similar to the spectra of ^{55}Fe and ^{3}H.

Finally, another important observation: when the spectra mixtures ^{3}H-^{55}Fe are analyzed applying the deconvolution method of Grau Carles [68], increasing chemical quench, the deconvolution is impossible due to the similarity of the spectral shapes.

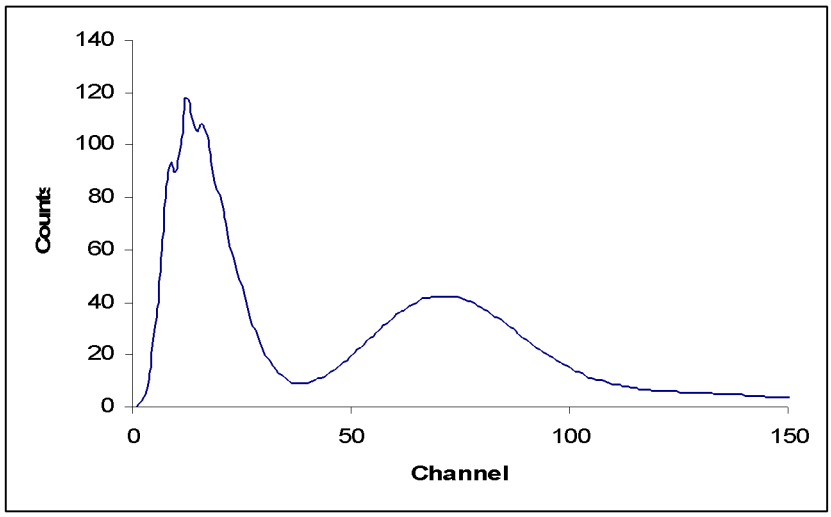

Fig. 9.- Spectrum of I-125. The low part of the spectrum is alike the spectra of ^{3}H, and ^{55}Fe.

3. Spectrometers with two photomultipliers

Commercial spectrometers have two photomultipliers placed in front of the sample with an angle of 180º. The photomultipliers are in coincidence, to reduce electronic noise and after-pulses, and in sum to recover the signal that has been distributed between both photomultipliers.

Table 1a.- Statistical factors for two photomultipliers with equal response. $(\bar{n}_1 = \bar{n}_2 = \bar{n})$

Operation mode	Statistical factor
A_1, A_2	$\sum_{n=1}^{\infty} P(n, 2\bar{n})(1-2^{-n})$
$A_1 + A_2$	$\sum_{n=1}^{\infty} P(n, 2\bar{n})$
$A_1 A_2$	$\sum_{n=2}^{\infty} P(n, 2\bar{n})(1-2^{1-n})$

Table 1b.- Statistical factor for two photomultipliers with different response. $(\bar{n}_1 \neq \bar{n}_2)$

Operation mode	Statistical factor
A_1	$\sum_{n=1}^{\infty} P(n, \bar{n}_1 + \bar{n}_2) - e^{-\bar{n}_1} \sum_{n=1}^{\infty} P(n, \bar{n}_2)$
$A_1 + A_2$	$\sum_{n=1}^{\infty} P(n, \bar{n}_1 + \bar{n}_2)$
$A_1 A_2$	$\sum_{n=2}^{\infty} P(n, \bar{n}_1 + \bar{n}_2) - e^{-\bar{n}_1} \sum_{n=2}^{\infty} P(n, \bar{n}_2) - e^{-\bar{n}_2} \sum_{n=2}^{\infty} P(n, \bar{n}_1)$

Tables 1a and 1b show the statistical factors to compute the pulse-height spectrum. Table 1a gives the equations when the two photomultiplier have the same output [99]. In other terms the mean number of photoelectrons at the photocathode is the same $(\bar{n}_1 = \bar{n}_2 = \bar{n})$. Table 1b presents, for the first time, the statistical factor to compute the pulse-height spectrum when the response of the photomultipliers is different $(\bar{n}_1 \neq \bar{n}_2)$.

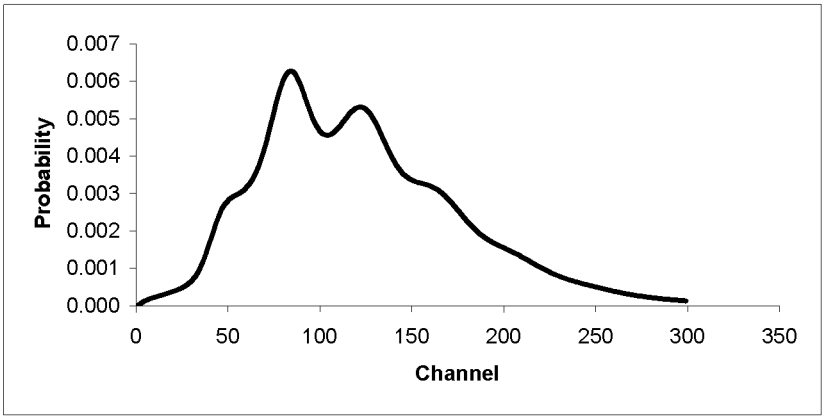

Fig. 10.- Spectrum for a monoenergetic sample producing a mean of 3 electrons at the photocathode output.

The equation to compute the spectrum for two photomultipliers in coincidence when $\bar{n}_1 = \bar{n}_2 = \bar{n}$ is:

$$S_i(2\bar{n}) = \sum_{n=2}^{\infty} \sum_{i=1}^{\infty} P(n,2\bar{n})(1-2^{1-n}) y_i^{(n)} \qquad (8)$$

where $2\bar{n}$ is the mean number of photoelectrons distributed among the two photomultipliers.

Fig. 10 shows a calculated spectrum taking $m = 3$ electrons. The peak of "monos" has disappeared due to the coincidence. We see two clear peaks. The first one corresponds to the coincidence of one electron from each photomultiplier. The second one corresponds to the emission of two photoelectrons from one of the photomultipliers and one photoelectron from the other photomultiplier. The hump on the first peak is due to the asymmetry of monos spectrum, see Fig. 2. Commercial spectrometers with two photomultipliers cannot be considered high resolution spectrometers because the spectrum of monos is very different from high resolution one shown in Fig. 1. We will analyse the behaviour of this type of spectrometers in a next paper.

4. Spectrometers with three photomultipliers

These spectrometers are not commercial and they are present in specialized radionuclide standardization laboratories. They use the well known TDCR (Triple Double Counting Rate) method. Fig. 11 shows three spectra of ^{55}Fe:

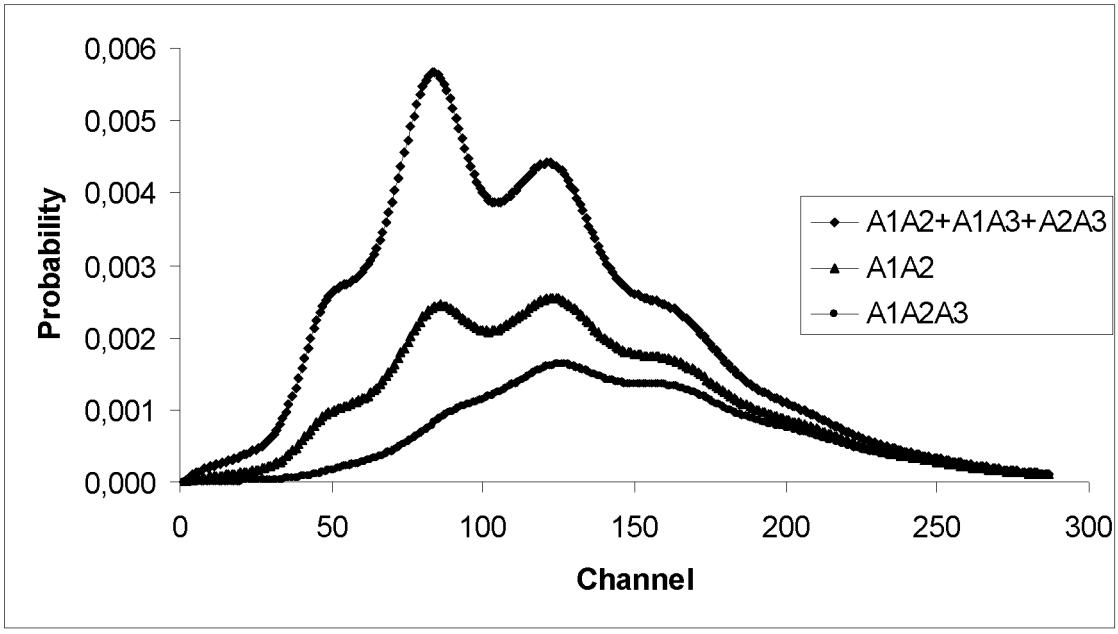

Fig. 11.- Spectra of ^{55}Fe obtained with a spectrometer with 3 photomultipliers in double coincidence sum $A_1A_2 + A_2A_3 + A_1A_3$, double coincidence A_1A_2, and triple coincidence: $A_1A_2A_3$.

1) Spectrum obtained with double coincidences ($A_1A_2 + A_1A_3 + A_2A_3$). The equation used is:

$$S_i(3\bar{n}) = \sum_{n=2}^{\infty}\sum_{i=1}^{\infty} P(n,3\bar{n})(1-3^{1-n})y_i^{(n)} \qquad (9)$$

2) Spectrum obtained with the coincidence of two photomultipliers (A_1A_2). The equation is:

$$S_i(3\bar{n}) = \sum_{n=2}^{\infty}\sum_{i=1}^{\infty} P(n,3\bar{n})[1-3^{-n}(2^{n+1}-1)]y_i^{(n)} \qquad (10)$$

3) Spectrum obtained with the coincidence of three photomultipliers ($A_1A_2A_3$). The equation used is:

$$S_i(3\bar{n}) = \sum_{n=3}^{\infty}\sum_{i=1}^{\infty} P(n,3\bar{n})[1-3^{1-n}(2^{n}-1)]\, y_i^{(n)} \qquad (11)$$

where $3\bar{n}$ is the mean number of photoelectrons distributed among the three photomultipliers.

Table 2a. Statistical factor for three photomultipliers with equal response. $(\bar{n}_1 = \bar{n}_2 = \bar{n})$

Operation mode	Statistical factor
$A_1; A_2$	$\sum_{n=1}^{\infty} P(n,3\bar{n})(1-3^{-n}2^{n})$
$A_1 + A_2$	$\sum_{n=1}^{\infty} P(n,3\bar{n})(1-3^{-n})$
$A_1 + A_2 + A_3$	$\sum_{n=1}^{\infty} P(n,3\bar{n})$
A_1A_2	$\sum_{n=2}^{\infty} P(n,3\bar{n})[1-3^{-n}(2^{n+1}-1)]$
$A_1A_2 + A_1A_3$	$\sum_{n=2}^{\infty} P(n,3\bar{n})[1-3^{-n}(2^{n}+1)]$
$A_1A_2 + A_1A_3 + A_2A_3$	$\sum_{n=2}^{\infty} P(n,3\bar{n})(1-3^{1-n})$
$A_1A_2A_3$	$\sum_{n=2}^{\infty} P(n,3\bar{n})[1-3^{1-n}(2^{n}-1)]$

Table 2a shows the equations to compute the statistical factor when the response of the three photomultipliers is statistically identical ($\bar{n}_1 = \bar{n}_2 = \bar{n}_3 = \bar{n}$) [99]. Table 2b shows the equations to compute the statistical factor when the three photomultipliers response is statistically different ($\bar{n}_1 \neq \bar{n}_2 \neq \bar{n}_3$).

Table 2b. Statistical factor for three photomultipliers with different response. ($\bar{n}_1 \neq \bar{n}_2 \neq \bar{n}_3$)

Operation mode	Statistical factor
A_1	$\sum_{n=1}^{\infty} P(n, \bar{n}_1 + \bar{n}_2 + \bar{n}_3) - e^{-\bar{n}_1} \sum_{n=1}^{\infty} P(n, \bar{n}_2 + \bar{n}_3)$
$A_1 + A_2$	$\sum_{n=1}^{\infty} P(n, \bar{n}_1 + \bar{n}_2 + \bar{n}_3) - e^{-(\bar{n}_1+\bar{n}_2)} \sum_{n=1}^{\infty} P(n, \bar{n}_3)$
$A_1 + A_2 + A_3$	$\sum_{n=1}^{\infty} P(n, \bar{n}_1 + \bar{n}_2 + \bar{n}_3)$
$A_1 A_2$	$\sum_{n=2}^{\infty} P(n, \bar{n}_1 + \bar{n}_2 + \bar{n}_3) + e^{-(\bar{n}_1+\bar{n}_2)} \sum_{n=2}^{\infty} P(n, \bar{n}_3)$ $- e^{-\bar{n}_1} \sum_{n=2}^{\infty} P(n, \bar{n}_2 + \bar{n}_3) - e^{-\bar{n}_{21}} \sum_{n=2}^{\infty} P(n, \bar{n}_1 + \bar{n}_3)$
$A_1 A_2 + A_1 A_3$	$\sum_{n=2}^{\infty} P(n, \bar{n}_1 + \bar{n}_2 + \bar{n}_3) + e^{-(\bar{n}_2+\bar{n}_3)} \sum_{n=2}^{\infty} P(n, \bar{n}_1)$ $- e^{-\bar{n}_1} \sum_{n=2}^{\infty} P(n, \bar{n}_2 + \bar{n}_3)$
$A_1 A_2 + A_1 A_3 + A_2 A_3$	$\sum_{n=2}^{\infty} P(n, \bar{n}_1 + \bar{n}_2 + \bar{n}_3) + e^{-(\bar{n}_1+\bar{n}_2)} \sum_{n=2}^{\infty} P(n, \bar{n}_3)$ $- e^{-(\bar{n}_1+\bar{n}_3)} \sum_{n=2}^{\infty} P(n, \bar{n}_2) - e^{-(\bar{n}_{21}+\bar{n}_3)} \sum_{n=2}^{\infty} P(n, \bar{n}_1)$
$A_1 A_2 A_3$	$\sum_{n=2}^{\infty} P(n, \bar{n}_1 + \bar{n}_2 + \bar{n}_3) + e^{-(\bar{n}_1+\bar{n}_2)} \sum_{n=2}^{\infty} P(n, \bar{n}_3)$ $- e^{-(\bar{n}_1+\bar{n}_3)} \sum_{n=2}^{\infty} P(n, \bar{n}_2) - e^{-(\bar{n}_{21}+\bar{n}_3)} \sum_{n=2}^{\infty} P(n, \bar{n}_1)$ $- e^{-\bar{n}_1} \sum_{n=2}^{\infty} P(n, \bar{n}_2 + \bar{n}_3) - e^{-\bar{n}_2} \sum_{n=2}^{\infty} P(n, \bar{n}_1 + \bar{n}_3)$ $e^{-\bar{n}_{31}} \sum_{n=2}^{\infty} P(n, \bar{n}_1 + \bar{n}_2)$

We understand here by different response when the spectrum of monos has the same shape but different amplitude for each one of the photomultipliers response. This one is the habitual case in which the three photomultipliers belong to the same company and model. When the spectra of monos are different in shape the problem become more complicated and will not be considered here.

An important point is the effect of the discriminator that eliminates photomultiplier electronic noise. This discriminator distorts the spectrum in the region of low energies. It is natural to suppose that a reduction of the efficiency takes place. Table 3 shows the discrepancies among the corrected and not corrected efficiency by the discriminator effect. The first column gives the TDCR. Columns 2, 3 and 4 show the discrepancies for

Table 3.- Activity losses for the discriminator that eliminates the electronic noise and possible counts of the radionuclide spectrum.

TDCR	Discrepancia %		
	Discrim. 10 canales	Discrim. 20 canales	Discrim. 30 canales
0.341	0.21	0.70	1.52
0.189	0.47	1.29	2.76
0.130	0.51	1.65	3.42
0.0989	0.58	1.86	3.83
0.0794	0.61	1.97	4.10
0.0666	0.65	2.08	4.29
0.0572	0.68	2.14	4.44
0.0502	0.70	2.23	4.55
0.0457	0.72	3.01	4.64

a discriminator level of 10, 20 and 30 channels, respectively. The first peak of coincidence is in channel 85. The positions of the discriminator in electrons are 0.24, 0.47 and 0.71, respectively. Since the discriminator diminishes the counting rate, the final result is a reduction of the calculated activity. This activity reduction may explain the discrepancies in some percents for ^{55}Fe and H-3 described in several papers [32, 49, 83, and 107].

5. Different Fe-55 spectra

In this section we present the computed spectra of ^{55}Fe for different spectrometer systems y different number of active photomultipliers. The free parameter for all the computations is $\lambda = 1.32$ KeV/electron.

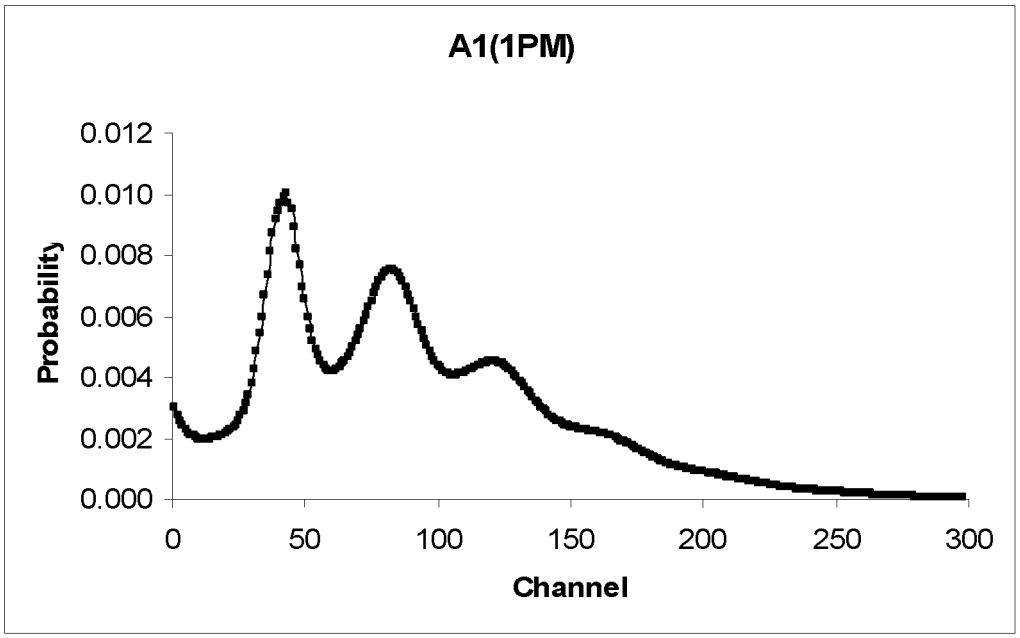

Fig. 12.- Spectrum of ^{55}Fe computed for a system with a unique photomultiplier.

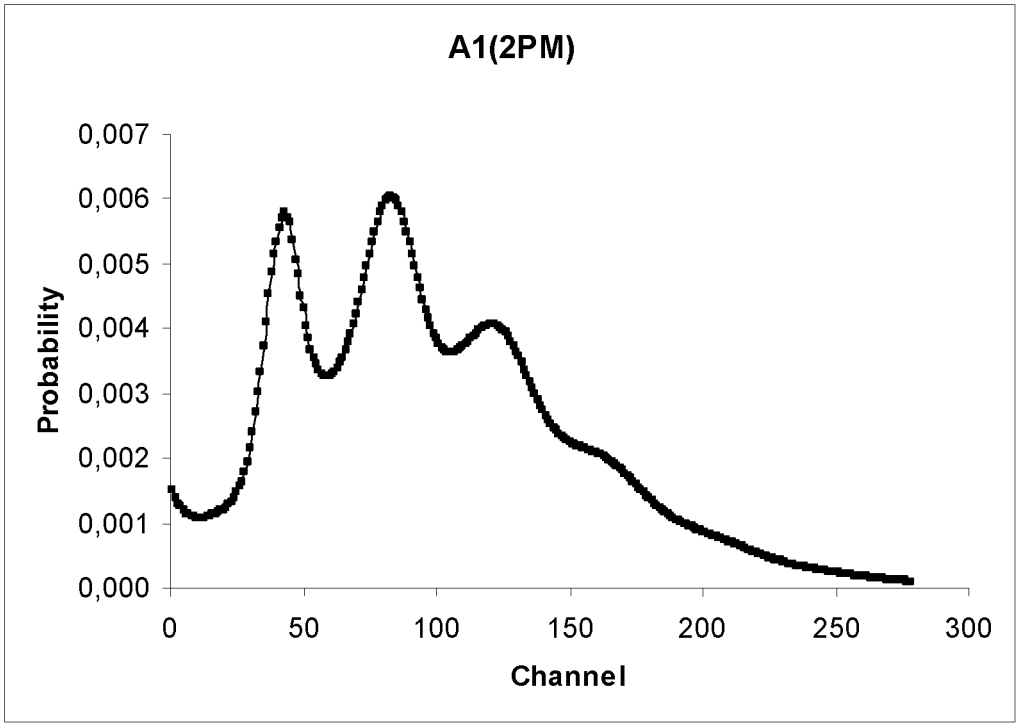

Fig. 13.- Spectrum of ^{55}Fe obtained with a photomultiplier with a system with two photomultipliers

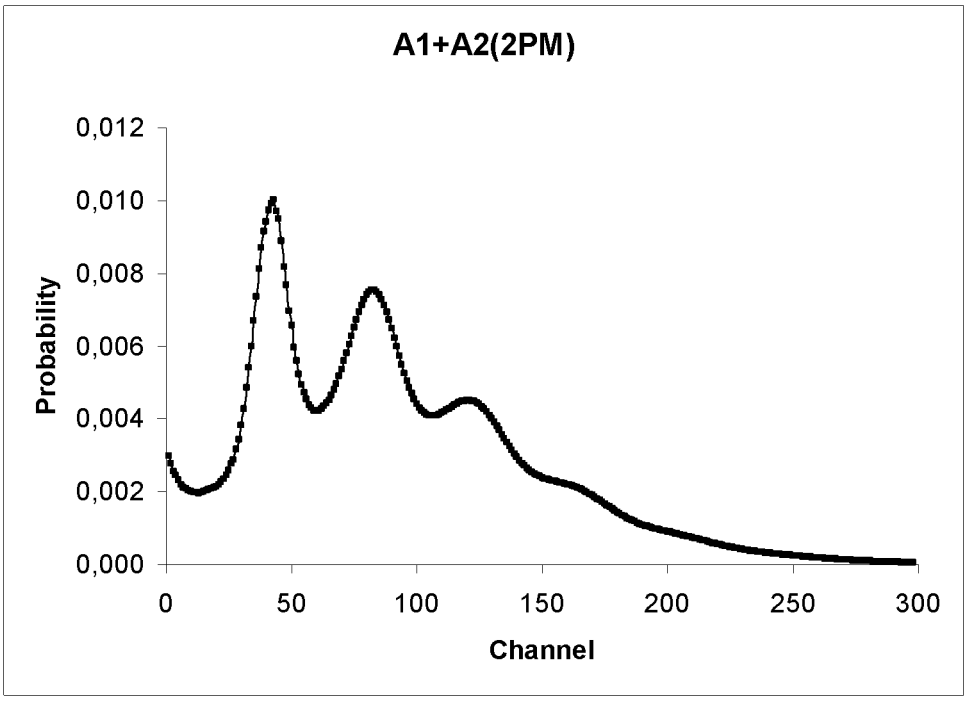

Fig. 14.- Spectrum of ^{55}Fe obtained with two photomultiplier working in addition with a system with two photomultipliers

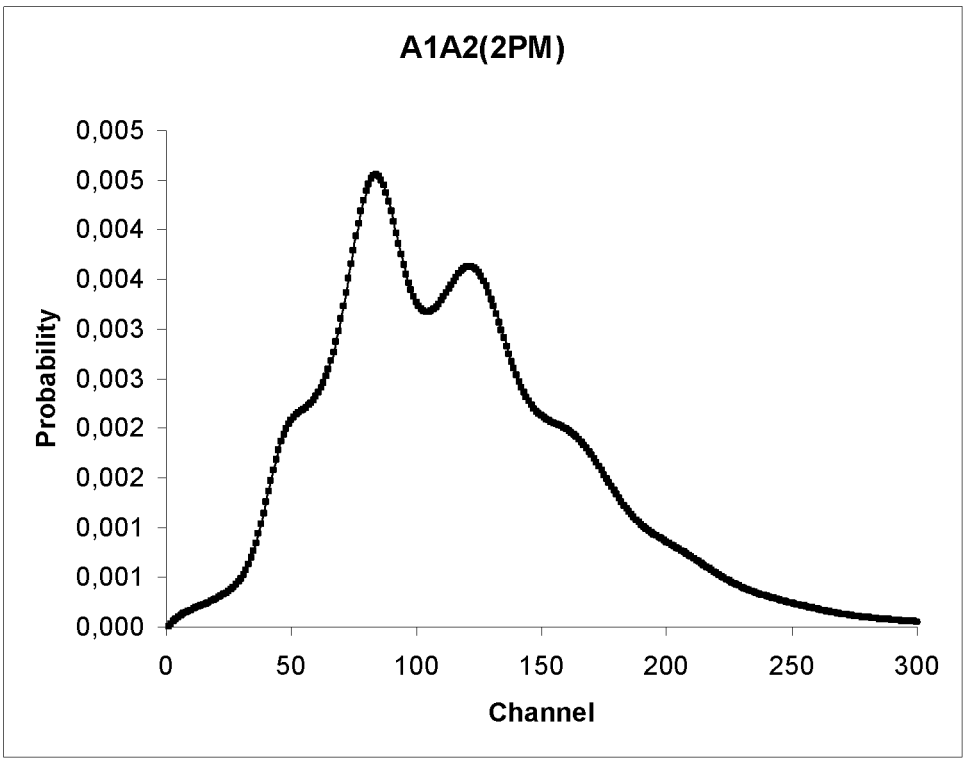

Fig. 15. Spectrum of ^{55}Fe obtained with two photomultiplier in coincidence with a system with two photomultipliers

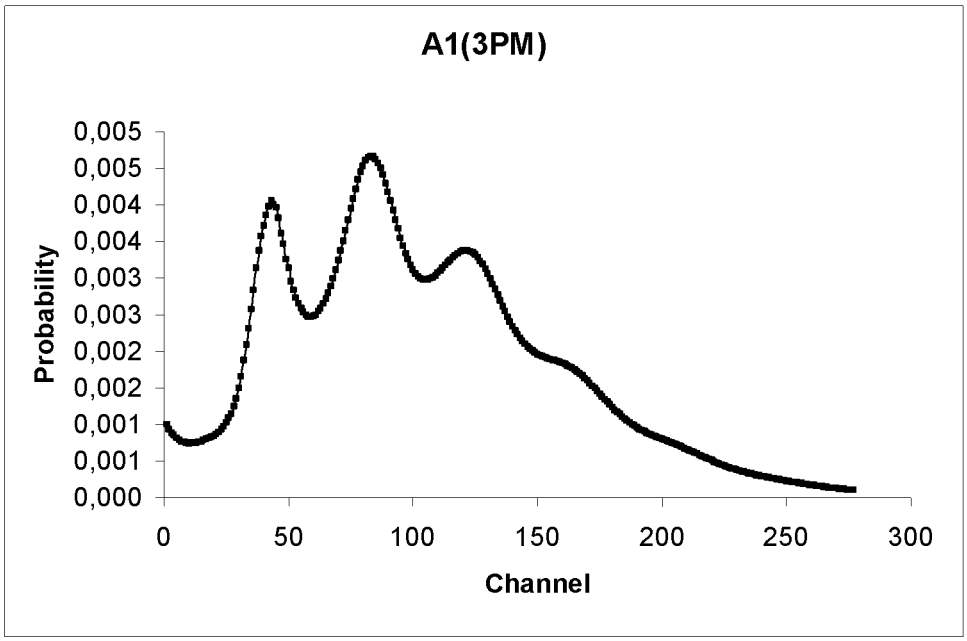

Fig. 16.- Spectrum of ^{55}Fe obtained with one photomultiplier with a three photomultipliers system.

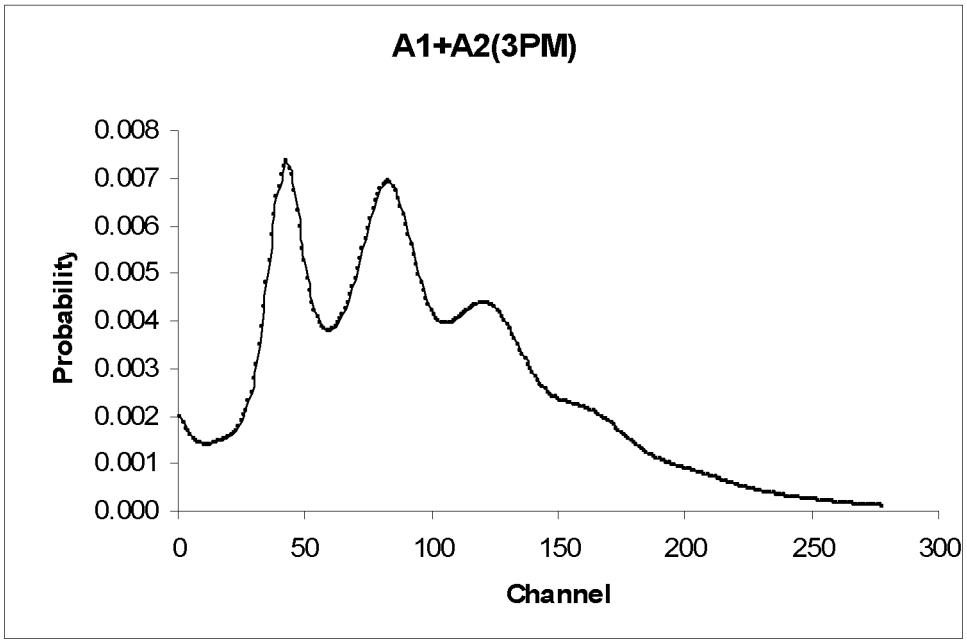

Fig. 17.- Spectrum of ^{55}Fe computed for two photomultipliers working in addition in a three photomultipliers system.

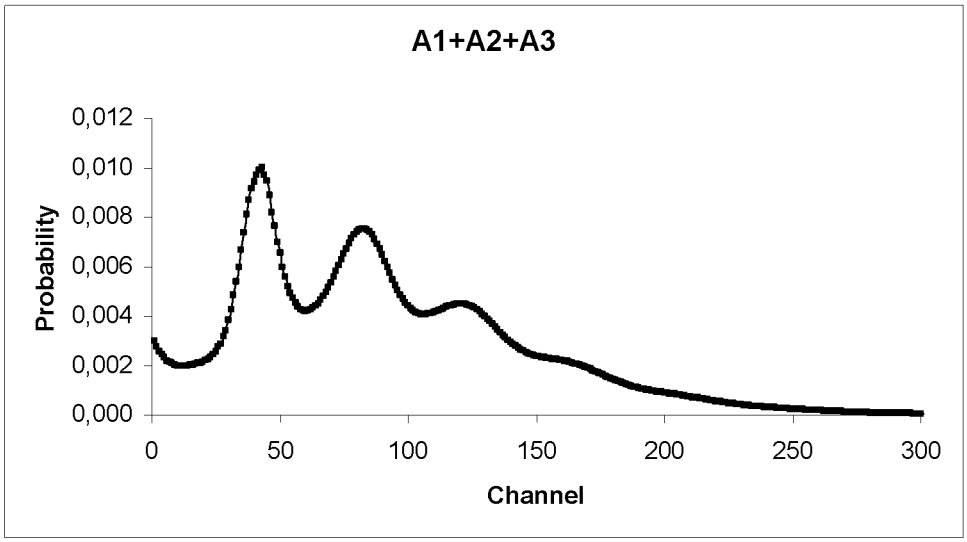

Fig. 18.- Spectrum of ^{55}Fe computed for three photomultipliers working in addition in a three photomultipliers system.

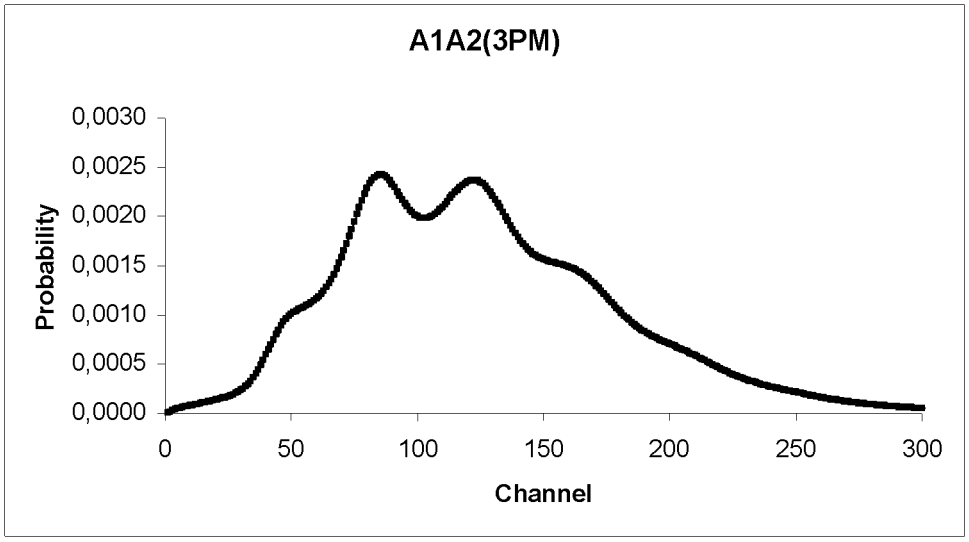

Fig. 19.- Spectrum of ^{55}Fe computed for two photomultipliers working in coincidence in a three photomultipliers system

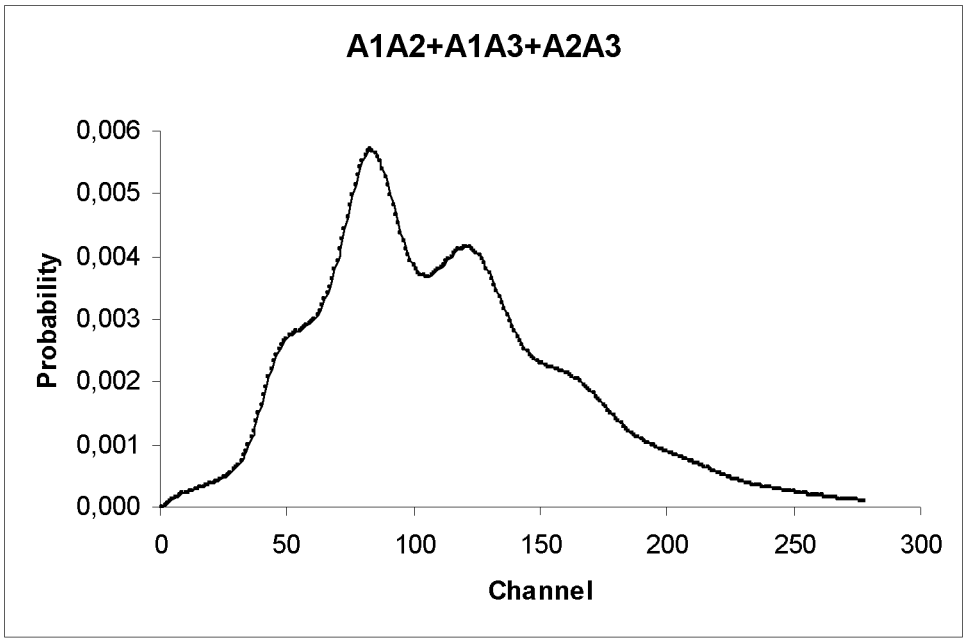

Fig. 19.- Spectrum of ^{55}Fe computed for two photomultipliers working in coincidence and addition in a three photomultipliers system

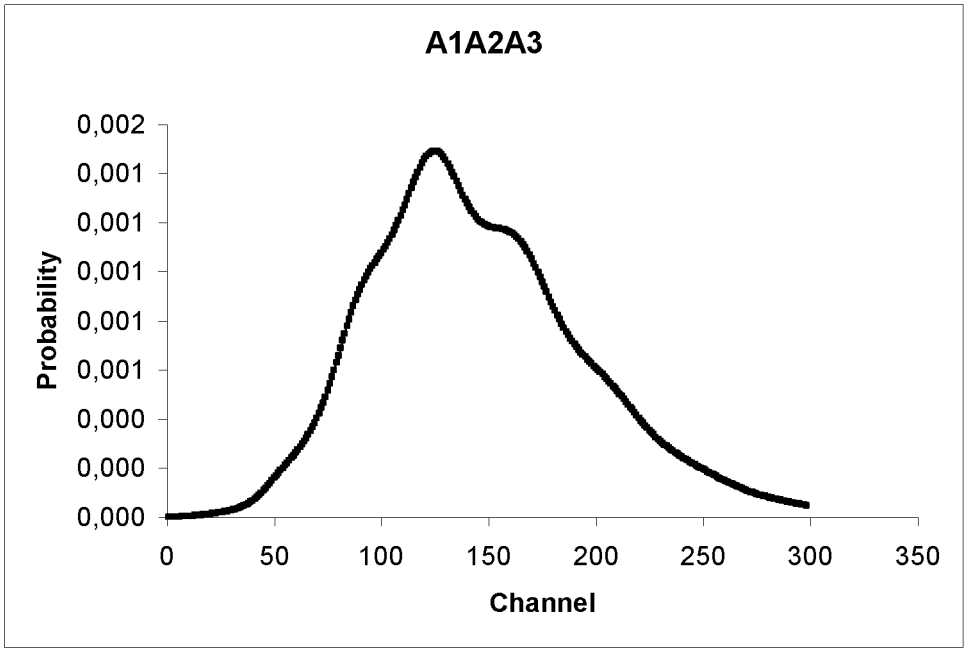

Fig. 20.- Spectrum of ^{55}Fe computed for three photomultipliers working in coincidence in a three photomultipliers system.

Fig. 12, 13 and 16 show the spectral response of one photomultiplier. The responses are quite different. The heights of the peaks are different: higher for Fig.12 and lower for Fig. 16. In Fig. 12 we show the spectrum for a detector with only one photomultiplier. In this case all the emitted light is arriving to the photomultiplier. In Fig. 13 we show the spectrum for a detector with two photomultipliers, when only one

of them is active. The emitted light is shared by the two photomultipliers, receiving each one only one-half of the light. In Fig. 16 the detector has three photomultipliers and the light received by one of them is one-third of the total. Fig. 17 and 18 show the spectra when the photomultipliers work in sum. In this case the first peak due to monos is reinforced compared with the second peak. Fig. 19 shows the spectrum for the coincidence of signals due to two photomultipliers. The peak of monos has disappeared. The small hump at the left of the principal peak is produced by the shape of the peak when $n = 2$ in Fig. 2. Fig. 19 shows the spectrum when the photomultipliers work in coincidence and addition. The firs peak has been reinforced for the photomultiplier addition process. Finally, Fig. 20 shows the spectrum for triple coincidence. In this case the peaks are produced by signals for $n \geq 3$ in Fig. 2. The contributions of $n = 3$ and $n = 4$ are the most important.

6. Conclusions

In this paper we describe a procedure to calculate the spectrum obtained with 1, 2 and 3 photomultipliers working in different coincidence ways. The emitter can be any radionuclide decaying by beta-ray emission or electron capture. The procedure has been applied to ^{55}Fe and the contribution of the after-pulses has been quantified for a single photomultiplier.

The influence of the free parameter and the kB in the spectrum peaks has been studied in the case of ^{55}Fe. We propose a procedure to fix the kB value and to obtain the same counting efficiency and the same spectrum when the free parameter is taken adequately.

We give the equations to calculate the statistical factor for two or three photomultiplier spectrometers and different operation ways when the outputs of the photomultipliers are different.

We have analysed the influence of the discriminators, which reduce the electronic noise, in the determination of the activity in a sample of ^{55}Fe.

An important conclusion is that the position of the peaks, in the low energy of the spectra obtained by liquid scintillation, is not characteristic of the particles energy interacting with the liquid scintillator, but the response of the photomultiplier.

7. References

[1] A. Grau Malonda, and E. García-Toraño. Evaluation of counting efficiency in liquid scintillation counting of pure b-ray emitters. *Int. J. Appl. Radiat. Isot.* **33** (1982) 249-253.

[2] A. Grau Malonda. Counting efficiency for electron capturing nuclides in liquid scintillation solution. *Int. J. Appl. Radiat. Isot.* **33** (1982) 371-375.

[3] A. Grau Malonda, E. García-Toraño, and J.M. Los Arcos. Liquid-scintillation counting efficiency as a function of the figure of merit for pure beta particle-emitters. *Int. J. Appl. Radiat. Isot.* **36** (1985) 157-158.

[4] B. M. Coursey, W. B. Mann, A. Grau Malonda, E. García-Toraño, J.M. Los Arcos, J. A. B. Gibson, and D. Reher. Standardization of carbon-14 by $4\pi\beta - \gamma$ liquid scintillation efficiency tracing with hydrogen-3. *Appl. Radiat. Isot.* **37** (1986) 403-408.

[5] A. Grau Malonda, and B. M. Coursey. Standardization of isomeric-transition radionuclides by liquid scintillation efficiency tracing with hydrogen-3: application to Technetium-99m. *Appl. Radiat. Isot.* **38** (1987) 695-700.

[6] R. Broda, K. Pochwalski, and T. Rodoszewski. Calculation of liquid-scintillation detector efficiency. *Appl. Radiat. Isot.* **39** (1988) 159-164.

[7] A. Grau Malonda, and B. M. Coursey. Calculation of beta-particle counting efficiency for liquid-scintillation systems with three photomultipliers. *Appl. Radiat. Isot.* **39** (1988) 1191-1196.

[8] B. R. S. Simpson, and B. R. Meyer. A multiple-channel 2- and 3-fold coincidence counting system for radionuclide standardization of low energy β-emitters. *Nucl. Instrum. Methods Phys. Res. Sect.* A **263** (1988) 346-440.

[9] A. Grau Carles, and A. Grau Malonda. Electron-capture standardization with a triple phototube system. *An. Fís., Ser. B* **85** (1989) 160-173.

[10] P. Cassette, and R. Vatin. Experimental evaluation of TDCR models for the 3 PM liquid scintillation counter. *Nucl. Instrum. Methods Phys. Res. Sect. A* **312** (1992) 95-99.

[11] B. M. Coursey, L. L. Lucas, A. Grau Malonda, and E. García-Toraño. The standardization of plutonium-241 and nikel-63. *Nucl. Instrum. Methods Phys. Res. Sect. A* **279** (1989) 603-610.

[12] B. M. Coursey, J. Cessna, E. García Toraño, D. B. Golas, A. Grau Malonda, D. H. Gray, D. D. Hopes, J. M. Los Arcos, M. T. Martin-Casallo, F. J. Shima, and M.P. Unterweger. The standardization and decay scheme Rhenium-186. *Appl. Radiat. Isot.* **42** (1991) 865-869.

[13] J. M. Calhoun, B. M. Coursey, D. Gray, and L. Karam. Standardization of ^{35}S methionine by liquid scintillation efficiency tracing with ^{3}H. In "Liquid Scintillation

Counting and Organic Scintillators" (H. Ross, J. E. Noakes and J. Spaulding, Eds.) pp 317-323 (1991). Lewis Publisher, Chelsea. MI 48118.

[14] B. R. S. Simpson, and B. R. Meyer. Further investigation of the TDCR efficiency calculation technique for the direct determination of the activity. *Nucl. Instrum. Methods Phys. Res. Sect. A* **312** (1992) 90-94.

[15] L. Rodríguez, J. M. Los Arcos, and A. Grau. LSC standardization of ^{54}Mn in inorganic and organic samples by the CIEMAT/NIST efficiency tracing method. *Nucl. Instrum. Methods Phys. Res. Sect. A* **312** (1992) 124-131.

[16] E. Günther, and U. Schötzing. Activity determination of ^{93m}Nb. *Nucl. Instrum. Methods Phys. Res. Sect. A* **312** (1992) 132-135.

[17] R. Broda, and K. Pochwalski. The TDCR method of standardizing ^{55}Fe and ^{54}Mn. In "Liquid Scintillation Spectrometry 1992" (J. E. Noakes, F. Schönhofer and H. A. Polach, Eds.) pp 255-260. *Radiocarbon* (1993). Tucson. USA.

[18] L. Rodríguez, J. M. Los Arcos, A. Grau Malonda, and E. García-Toraño. LSC standardization of ^{45}Ca by the CIEMAT/NIST efficiency tracing method. *Nucl. Instrum. Methods Phys. Res. Sect. A* **339** (1994) 6-13.

[19] B. R. S. Simpson, and B. R. Meyer. Direct activity measurement of pure beta-emitting radionuclides by the TDCR efficiency calculation technique. *Nucl. Instrum. Methods Phys. Res. Sect. A* **339** (1994) 14-20.

[20] B. M. Coursey, J. M. Calhoun, J. Cessna, D. B. Golas, and F. J. Shima. Liquid scintillation counting techniques for the standardization of radionuclides used in therapy. *Nucl. Instrum. Methods Phys. Res. Sect. A* **339** (1994) 26-30.

[21] B. R. S. Simpson, and B. R. Meyer. Standardization and half-life of ^{201}Tl by the $4\pi(x,e)-\gamma$ coincidence method with liquid scintillation counting in the 4π -channel. *Appl. Radiat. Isot.* **45** (1994) 669-673.

[22] B. R. S. Simpson, and B. R. Meyer. Activity measurement of ^{204}Tl by direct liquid scintillation measurements. *Nucl. Instrum. Methods Phys. Res. Sect. A* **369** (1996) 340-343.

[23] L. Rodríguez Barquero, and J. M. Los Arcos. ^{41}Ca standardization by the CIEMAT/NIST LSC method. *Nucl. Instrum. Methods Phys. Res. Sect. A* **369** (1996) 353-358.

[24] B. M. Coursey, F. J. Shima, D. B. Golas, O. T. Palabrica, A. Suzuki, and M. A. Dell. Measurement standards for strontium-89 for use in bone palliation. *Appl. Radiat. Isot.* **49**(4) (1998) 335-344.

[25] R. Broda, M. N. Peron, P. Cassette, T. Terlikowska, and D. Hainos. Standardization of ^{139}Ce by liquid scintillation counting using the triple top double coincidence ratio method. *Appl. Radiat. Isot.* **49** (9-11) (1998) 1035-1040.

[26] B. R. S. Simpson, and B. R. Meyer. Activity measurement of ^{55}Fe by an efficiency calculation method. *Appl. Radiat. Isot.* **49** (9-11) (1998) 1073-1076.

[27] L. Rodríguez Barquero, J. M. Los Arcos, F. Ortiz, and A. Jiménez. ^{49}V Standardization by the CIEMAT/NIST LSC method. *Appl. Radiat. Isot.* **49** (9-11) (1998) 1077-1082.

[28] P. Cassette, T. Altzitzoglou, R. Broda, R. Colle, P. Dryac, P. De Felice, E. Günther, J. M. Los Arcos, G. Ratel, B. Simpson, and F. Verregen. Comparison of activity concentration measurement of ^{63}Ni and ^{55}Fe in the framework of the EUROMET 297 project. *Appl. Radiat. Isot.* **49** (1998) 1403-1410.

[29] A. Ceccatelli, and P. De Felice. Standardization of ^{90}Sr, ^{63}Ni and ^{55}Fe by the $4\pi\beta$ liquid scintillation spectrometry method with ^{3}H-standard efficiency tracing. *Appl. Radiat. Isot.* **51** (1999) 85-92.

[30] E. Günther. Standardization of ^{207}Np by the CIEMAT/NIST LSC tracer method. *Appl. Radiat. Isot.* **52** (2000) 471-474.

[31] E. García-Toraño, M. Roteta, and L. Rodríguez Barquero. Standardization of ^{110m}Ag by liquid scintillation and $4\pi\beta-\gamma$ counting coincidence. *Appl. Radiat. Isot.* **52** (2000) 637-641.

[32] P. Cassette, R. Broda, D. Hainos, and T. Terlikowska. Analysis of detection-efficiency variation techniques for the implementation of the TDCR method in liquid scintillation counting. *Appl. Radiat. Isot.* **52** (2000) 643-648.

[33] B. E. Zimmermann, M. P. Unterweger, and J. W. Brodack. The standardization of ^{77}Lu by $4\pi\beta$ liquid scintillation spectrometry with ^{3}H-standard efficiency tracing. *Appl. Radiat. Isot.* **54** (2001) 623-631.

[34] E. Günther. Determination of the ^{32}P activity in angioplastic balloons by LSC. *Appl. Radiat. Isot.* **56** (2002) 291-293.

[35] B. R. S. Simpson, and W. M. Morris. The standardization of ^{33}P by the TDCR efficiency calculation technique. *Appl. Radiat. Isot.* **60** (2004) 465-468.

[36] Han-Yull Hwang, Seon-Im Kwak, Hwa Young Lee, Jong-Man Lee, Kyung-Beom Lee, and Tae Soon Park. Development of 3-PM liquid scintillation counting system with geometrical efficiency variation. *Appl. Radiat. Isot.* **60** (2004) 465-468.

[37] K. Kossert, and A. Grau Carles. The LSC efficiency for low-Z electron-capture nuclides. *Appl. Radiat. Isot.* **64** (2006) 1446-1453.

[38] W. M. van Wyngaardt, and B. R. S. Simpson. Absolute activity measurement of the electron-capture-based radionuclides ^{139}Ce, ^{125}I, ^{192}Ir and ^{65}Zn by liquid scintillation coincidence counting. *Appl. Radiat. Isot.* **64** (2006) 1454-1458.

[39] K. Kossert. A new method for secondary standard measurements with the aid of liquid scintillation counting. *Appl. Radiat. Isot.* **64** (2006) 1459-1464.

[40] P. Cassette, G. H. Ahn, T. Alzitzoglou, I. Aubineau-Lanièce, F. Bochud, E. García-Toraño, A. Grau Carles, A. Grau Malonda, K. Kossert, K. B. Lee, J. P. Laedermann. B. R. S. Simpson, W. M. van Wyngaardt, and B. E. Zimmerman. Comparison of calculated spectra for the interaction of photons in a liquid scintillator. Example of ^{54}Mn 835 keV emission. *Appl. Radiat. Isot.* **64** (2006) 1471-1480.

[41] B. R. S. Simpson, and W. M. van Wyngaardt. Activity measurement of the high-energy pure β-emitters ^{89}Sr and ^{90}Y by the TDCR efficiency calculation technique. *Appl. Radiat. Isot.* **64** (2006) 1481-1484.

[42] K. Kossert, and A. Grau Carles. Study of a Monte Carlo rearrangement model for the activity determination of electron-capture nuclides by means of liquid scintillation counting. *Appl. Radiat. Isot.* **66** (2008) 998-1005.

[43] C. Ivan, P. Cassette, and M. Sahagia. A new TDCR-LS Counter using Channel photomultipliers tubes. *Appl. Radiat. Isot.* **66** (2008) 1006-1011.

[44] W. M. van Wyngaardt, B. R. S. Simpson, and G. E. Jackson. Further investigations of a simple counting technique for measuring mixtures of two pure β-emitting radionuclides. *Appl. Radiat. Isot.* **66** (2008) 1012-1020.

[45] P. Cassette, and P. Do. The Compton source efficiency tracing method in liquid scintillation counting: A new standardization method using a TDCR counter with a Compton spectrometer. *Appl. Radiat. Isot.* **66** (2008) 1026-1032.

[46] R. Broda. Some remarks on photons statistics in LS-counter. *Appl. Radiat. Isot.* **66** (2008) 1062-1066.

[47] M. F. L'Annunziata. Liquid Scintillation Analysis: Principles and Practice. Handbook of Radioactivity Analysis (Amsterdam: Academic Press). 2nd Edition (2003).

[48] NCRP. A handbook of radioactivity measurements procedures. Report no. 58. 1985.

[49] R. Broda, P. Cassette, and K. Kossert. Radionuclide metrology using liquid scintillation counting. *Metrologia*, **44** (2007) S36-S52.

[50] E. García Toraño, and A. Grau Malonda. EFFY, a program to calculate the counting efficiency of beta particles in liquid scintillation counting. *Comput. Phys. Commun.* **23** (1981) 385-391.

[51] E. García Toraño, and A. Grau Malonda. EFFY2, a new program to calculate the counting efficiency of beta particles in liquid scintillation counting. *Comput. Phys. Commun.* **36** (1985) 307-312.

[52] J. M. Los Arcos, A. Grau Malonda, and A. Fernandez. VIASKL: a computer program to evaluate the liquid scintillation counting efficiency and its associated uncertainty for K-L-atomic Shell electron-capture nuclides. *Comput. Phys. Commun.* **44** (1987) 209-220.

[53] A. Grau Carles, and A. Grau Malonda. EMI, the counting efficiency for electron capture, electron capture gamma and isomeric transitions. *Comput. Phys. Commun.* **79** (1994) 115-123.

[54] E. García Toraño, and A. Grau Malonda. EFYGA, a Monte Carlo program to compute the interaction probability and the counting efficiency of rays in liquid scintillators. *Comput. Phys. Commun.* **47** (1987) 341-347.

[55] E. García Toraño, A. Grau Malonda, and J. M. Los Arcos. EBEGA- the counting efficiency of a beta-gamma emitter in liquid scintillators. *Comput. Phys. Commun.* **50** (1988) 313-319.

[56] A. Grau Carles. SRLOG, the simultaneous standardization of ^{90}Sr+^{90}Y+^{89}Sr. *Comput. Phys. Commun.* **82** (1994) 17-22

[57] G. Galiano, A. Grau Carles, and A. Grau Malonda. CAPMULT, the counting efficiency for electron capture by KLMN four-shell model. *Comput. Phys. Commun.* **87** (1995) 432-437.

[58] A. Grau Carles. MLOG, the simultaneous standardization of multi-nuclide mixtures. *Comput. Phys. Commun.* **93** (1996) 49-52.

[59] J. M. Los Arcos, and F. Ortiz. KB: a code to determinate the ionization quench function Q(E) as a function of the kB parameter. *Comput. Phys. Commun.* **44** (1997) 83-94.

[60] A. Grau Malonda, A. Grau Carles, P. Grau Carles, and G. Galiano Casas. EMI2, the counting efficiency for electron capture by a $KL_1L_2L_3M$ model. *Comput. Phys. Commun.* **123** (1999) 114-122.

[61] R. Broda, P. Cassette, K. Maletka, and K. Pochwalski. A simple computing program for application of the TDCR method to standardization of pure-beta emitters. *Appl. Radiat. Isot.* **52** (2000) 673-678.

[62] A. Grau Carles. EMILIA, the liquid-scintillation counting efficiency for electron-capture and capture-gamma emitters. *Comput. Phys. Commun.* **174** (2006) 35-46.

[63] A. Grau Carles. MICELLE, the micelle size effect on the LS counting efficiency. *Comput. Phys. Commun.* **176** (2007) 305-317.

[64] D. Rodrigues, P. Arenillas, M. E. Capoulat, and C. Balpardo. General data analysis code for TDCR liquid scintillation counting. *Appl. Radiat. Isot.* **66** (2008) 1049-1054.

[65] A. Grau Carles, M. T. Martín-Casallo, and A. Grau Malonda. Spectrum unfolding and double window methods applied to standardization of ^{14}C and ^{3}H mixtures. *Nucl. Instrum. Methods Phys. Res. Sect. A* **307** (1991) 484-490.

[66] A. Grau Carles, and A. Grau Malonda. A new procedure for multiple isotope analysis in liquid scintillation counting. In "Liquid Scintillation counting and Organic Scintillators" (Harley Ross, John E. Noakes and Jim Spaulding, Eds.), (1992) pp 295-306. Lewis Publishers, Chelsea, MI 48118.

[67] A. Grau Carles, L. Rodriguez Barquero, and A. Grau Malonda. Standardization of ^{14}C and ^{35}S mixtures. *Nucl. Instrum. Methods Phys. Res. Sect. A* **335** (1993) 234-240

[68] A. Grau Carles. A new linear spectrum unfolding method applied method applied to radionuclide mixtures in liquid scintillation spectrometry. *Appl. Radiat. Isot.* **45** (1993) 83-90.

[69] A. Grau Carles, L. Rodriguez Barquero, and A. Grau Malonda. A spectrum unfolding method applied to standardization of ^{3}H and ^{55}Fe mixtures. *Appl. Radiat. Isot.* **44** (1993) 581-586.

[70] A. Grau Carles, L. Rodriguez Barquero, and A. Grau Malonda. Standardization of multi-nuclide mixtures by a new spectrum unfolding method. *J. Radioanal. Nucl. Chem. Letters* **176** (1993) 391-403.

[71] A. Grau Carles, L. Rodríguez Barquero, and A. Grau Malonda. Simultaneous standardization of $^{90}Sr-^{90}Y$ and ^{89}Sr mixtures. *Appl. Radiat. Isot.* **44** (1993) 1003-1010.

[72] A. Grau Carles, L. Rodriguez Barquero, and A. Grau Malonda. Double-label counting of heterogeneous samples. In "Liquid Scintillation Spectrometry 1992" (J. E. Noakes, F. Schönhofer and H. A. Polach, Eds.) *Radiocarbon*, 1993, 239-248.

[73] A. Grau Malonda, L. Rodríguez Barquero, and A. Grau Carles. Radioactivity determination of ^{90}Y, ^{90}Sr and ^{89}Sr mixtures by spectral deconvolution. *Nucl. Instrum. Methods Phys. Res. Sect. A* **339** (1994) 31-37.

[74] A. Grau Carles, L. Rodriguez Barquero, and A. Grau Malonda. Deconvolution of $^{204}Tl/^{36}Cl$ and $^{147}Pm/^{45}Ca$ dual mixtures. *Nucl. Instrum. Methods Phys. Res. Sect. A* **339** (1994) 71-77.

[75] A. Grau Carles, A. Grau Malonda, and V. Gómez Gil. Standardization of $U(X_1+X_2)$: the $^{234}Th+^{234m}Pa+^{230}Th$ mixture. *Nucl. Instrum. Methods Phys. Res. Sect. A* **369** (1994) 431-436.

[76] A. Grau Carles. MLOG, the simultaneous standardization of multi-nuclide mixtures. *Comput. Phys. Commun.* **93** (1996) 48-52.

[77] A. Grau Malonda, and A. Grau Carles. Half-life determination of ^{40}K by LSC. *Appl. Radiat. Isot.* **56** (2002) 153-156.

[78] K. Kossert, and E. Günther. LSC measurements of the half-life of ^{40}K. *Appl. Radiat. Isot.* **60** (2004) 459-464.

[79] A. Grau Carles. New Methods for the Determination of Beta Spectra Shape factors. *Appl. Radiat. Isot.* **46** (1995) 125-128.

[80] A. Grau Carles. Beta shape factor determination by the cutoff energy yield method. *Nucl. Instrum. Methods Phys. Res. Sect. A* **551** (2005) 312-322.

[81] A. Grau Carles, and K. Kossert. New advances in the determination of the ^{87}Rb shape factor function. *Nucl. Phys. A* **767** (2006) 248-258

[82] A. Grau Carles, K. Kossert, and A. Grau Malonda. Determination of the shape factor of ^{90}Sr by means of the cutoff energy yield method. *Appl. Radiat. Isot.* **66** (2008) 1021-1025.

[83] G. García, F. Blanco, A. Grau Carles, and A. Grau Malonda. Inelastic scattering and stopping Power of low-energy electrons (0.01-10 keV) in toluene. *Appl. Radiat. Isot.* **60** (2004) 481-485.

[84] A. Grau Carles. Synergic quenching effects of water and carbon tetrachloride on liquid-scintillation gel samples. *Appl. Radiat. Isot.* **64** (2006) 1505-1509.

[85] A. Grau Carles, and A. Grau Malonda. Alpha/Beta Separation in Liquid Scintillation Gel Samples. *Nucl. Instrum. Meth. Phys. Res. Sect. A* **345** (1994) 102-106.

[86] A. Grau Malonda, A. Grau Carles, and G. García. Mean values of the LMM Auger transition in a KLM model. *Appl. Radiat. Isot.* **64** (2006) 1485-1491.

[87] A. Grau Carles, and A. Grau Malonda. Precise system for the determination of the quench parameter of radioactive samples in liquid phase. Patent. 9202639. December 29, 1992. Register of the Industrial Property, Madrid, Spain.

[88] B. E. Zimmerman. Monte Carlo calculations of spectra and interaction probabilities for photons in liquid scintillators for use in the standardization of radionuclides. *Appl. Radiat. Isot.* **64** (2006) 1492-1498.

[89] A. Grau Carles, and A. Grau Malonda. Computational aspects in modelling the interaction of low-energy X-rays with liquid scintillators. *Appl. Radiat. Isot.* **64** (2006) 1515-1519.

[90] B. E. Zimmerman, R. Collé and J. T. Cessna. Construction and implementation of the NIST triple-to-double coincidence ratio (TDCR) spectrometer. *Appl. Radiat. Isot.* **60** (2004) 433-438.

[91] R. Broda, and A. Jeczmieniowski. Statistics of the LS-detector in the case of low counting efficiency. *Appl. Radiat. Isot.* **60** (2004) 453-458.

[92] A. C. Razdolescu, R. Broda, P. Cassette, B. R. S. Simpson, and W. M. Van Wyngaardt. The IFIN-HH triple coincidence liquid scintillation counter. *Appl. Radiat. Isot.* **64** (2006) 1510-1514.

[93] A. Grau Carles, L. Rodríguez Barquero, and A. Jiménez De Mingo. ^{125}Sb to ^{125m}Te branching ratio. *Appl. Radiat. Isot.* **49** (1998) 1377-1381.

[94] H. Houtermans. Probability of non-detection in liquid scintillation counting. *Nucl. Instrum. Methods*. **112** (1973) 121-130.

[95] P. B. Coates. The edge effect in electron multiplier statistics. *J. Phys. D. Appl. Phys.* **3** (1970) 1290-1296.

[96] P. Arenillas, and P. Cassette. Implementation of the TDCR liquid scintillation method at CNEA-LMR, Argentina. *Appl. Radiat. Isot.* **64** (2006) 1500-1504.

[97] M. J. Qin, L. Mo, D. Alexiev, and P. Cassette. Construction and implementation of a TDCR system at ANSTO. *Appl. Radiat. Isot.* **66** (2008) 1033-1037.

[98] A. Williams, and D. Smith. Afterpulses in liquid scintillation counters. *Nucl. Instrum. Methods* **112** (1973) 131-135

[99] A. Grau Malonda. "Free parameter models in liquid scintillation counting". Editorial CIEMAT. Madrid (1999). pp. 228-255.

[100] P. Grau Carles, and A. Grau Malonda. Free parameter, figure of merit and ionization quench in liquid scintillation counting. *Appl. Radiat. Isot.* **54** (2001) 447-454.

[101] G. García, and A. Grau Malonda. The influence of stopping power on the ionization quench factor. *Appl. Radiat. Isot.* **56** (2002) 295-300

[102] A. Grau Carles, E. Günther, G. García, and A. Grau Malonda. Ionization quenching in LSC. *Appl. Radiat. Isot.* **60** (2004) 447-451

[103] A. Grau Carles, E. Günther, and A. Grau Malonda. The photoionization reduced energy in LSC. *Appl. Radiat. Isot.* **64** (2006) 43-54.

[104] A. Grau Malonda, and A. Grau Carles. The ionization quench factor in liquid-scintillation counting standardizations. *Appl. Radiat. Isot.* **51** (1999) 183-188.

[105] A. Grau Malonda, and A. Grau Carles. The ionization quenching function for coincident electrons. *Appl. Radiat. Isot.* **66** (2008) 1043-1048.

[106] E. Günther. Standardization of the EC nuclides ^{55}Fe and ^{65}Zn with the CIEMAT/NIST LSC tracer method. Appl. Radiat. Isot. **49** (1998) 1055-1060.

[107] B. R. Meyer, and B. R. S. Simpson. A direct method for ^{55}Fe activity measurement. *Appl. Radiat. Isot.* **41** (1990) 375-379.